Commun. Comput. Phys.
doi: 10.4208/cicp.371011.260112s

Vol. **13**, No. 3, pp. 880-899
March 2013

A Lattice Boltzmann Model to Study Sedimentation Phenomena in Irrigation Canals

Olivier Marcou[1,*], Bastien Chopard[2], Samira El Yacoubi[1], Boussad Hamroun[3], Laurent Lefèvre[4] and Eduardo Mendes[4]

[1] *Institut de Modélisation et Analyse en Géo-Environnement et Santé, Université de Perpignan Via Domitia, Perpignan, France.*
[2] *Computer Science Department, University of Geneva, Switzerland.*
[3] *Laboratoire d'Automatique et de Génie des Procédés, Université Claude Bernard, Lyon, France.*
[4] *Laboratoire de Conception et Intégration des Systèmes, Grenoble INP, Valence, France.*

Received 31 October 2011; Accepted (in revised version) 26 January 2012

Available online 29 August 2012

Abstract. Fresh water is one of the most significant resources for human activities and survival, and irrigation is among the most important uses of water. The sustainibility and performance of irrigation canals can be greatly affected by sediment transport and deposition. In our previous works, we proposed a Lattice Boltzmann model for simulating a free surface flow in an irrigation canal, as an alternative to more traditional models mainly based on shallow water equations. Here we introduce the sedimentation phenomenon into our model by adding a new algorithm, based on the earlier work by B. Chopard, A. Dupuis and A. Masselot [9, 11, 12, 27]. Transport, erosion, deposition and toppling of sediments are taken into account and enable the global sedimentation algorithm to simulate different transport modes such as bed load and suspended load. In the present work, we study both the behaviour of a sediment deposit located at an underflow submerged gate (depending on the gate opening and the flow discharge) and the influence of the presence of such a deposit on the flow. Both numerical and experimental validations have been performed. The experiments were realized on the micro-canal of the LCIS laboratory at Valence, France. The comparisons between simulations and experiments give good qualitative agreement.

AMS subject classifications: 76T10, 76B07, 76D06, 76T20

Key words: Lattice Boltzmann method, irrigation canals modeling, sedimentation.

*Corresponding author. *Email addresses:* marcou@univ-perp.fr (O. Marcou), Bastien.Chopard@unige.ch (B. Chopard), yacoubi@univ-perp.fr (S. El Yacoubi), hamroun@lagep.cpe.fr (B. Hamroun), Laurent.Lefevre@lcis.grenoble-inp.fr (L. Lefèvre), Eduardo.Mendes@lcis.grenoble-inp.fr (E. Mendes)

1 Introduction

Nowadays, water resources are becoming more and more scarce. As the world population increases, so does the demand of fresh water, while the supplies are slowly decreasing due to various causes. Therefore, good management of water resources is a problem of increasing importance. Since one of the most important uses of water is irrigation, the development of efficient and optimal controllers for irrigation canals systems is a challenging engineering problem.

Various types of perturbations can affect irrigation canals. Among them, one can count sediment or algae transport and deposition. The topic of sedimentation in general covers a wide variety of situations and phenomena. The formation of ripples and dunes under various types of flow has been studied as well (for instance, in [17, 33, 34]). The general problem of erosion and transport in shallow water has also been treated by several authors (see, e.g., [2, 13]; see also [10] for a study on the structure and formation of sediment deposits in an experimental channel).

Sedimentation in irrigation canals cause various problems, usually resulting in a decrease in the discharge provided by the system, and affecting maintenance costs. Understanding and modeling the sedimentation processes is thus a necessity in order to improve control systems operating on irrigation canals. Predictors have been developed in order to calculate the sediment transport capacity for an irrigation canal. However, these methods are usually designed for a given set of situations and flow conditions, and even when used accordingly, their accuracy is limited [32].

In this work, we will propose an introductory study of sedimentation problems in the context of a LB modeling of an irrigation canal.

Irrigation canals are hydraulic systems where the flow dynamics is usually described with a set of partial differential equations which derives from the Navier-Stokes equations, and known as shallow water equations; they may also be called Saint-Venant (SV) equations. These equations can be expressed as follows:

$$B\frac{\partial h}{\partial t}+\frac{\partial Q}{\partial x}=0, \tag{1.1}$$

$$\frac{\partial Q}{\partial t}+B\frac{\partial h}{\partial x}\cdot\left(gh-\frac{Q^2}{h^2B^2}\right)+\frac{\partial Q}{\partial x}\cdot\frac{2Q}{Bh}+gBh\cdot(S_f-\bar{S})=0 \tag{1.2}$$

for all $(x,t)\in]0,L[\times R^+$ where x is the spatial location along the canal and t is the temporal variable; Q is the discharge, g the gravity, h the water elevation, B the width of the channel. The quantity $\bar{S}$ is the channel slope and S_f is the friction between the water and the canal walls.

Such equations are used for modeling the flow inside a given section of a canal. The different sections communicate through various types of gates. The behavior of these gates is also described by specific equations that basically define the boundary conditions of the previous SV equations. For instance, the following equation is a standard discharge

relationship for an immersed underflow gate:

$$Q = O \cdot B \cdot \theta \sqrt{2g(h_{up} - h_{down})}, \tag{1.3}$$

where h_{up} and h_{down} are the water levels respectively upstream and downstream of the gate, with $h_{up} > h_{down}$. The constant θ is a gate-specific coefficient. The quantity O is the opening of the gate.

In our previous studies [22–26], we proposed a Lattice Boltzmann model whose objective was to model and simulate flows in irrigation canals. The LB method offers several advantages. Its formulation and application are simpler when compared to more classical methods for solving Navier-Stokes equations. From a numerical point of view, the high locality of its algorithm makes LBM particularly adapted to computations on parallel processing systems. It also allows to easily include various additional phenomena, and has been successfully used for a wide variety of flows (multiphase flows, multi-scale flows, particle suspension$\cdots$).

In particular, in the context of irrigation canals, we investigated how the LB approach made it possible to simulate more accurately what happens in the vicinity of gates. Indeed, even though the gates separating the different sections of a canal are treated in classical models as boundary conditions, it is not the case in our LB model when gates located inside the simulated system are concerned: a gate between two reaches is simply modelled as an orifice in the wall separating those reaches, without need for using discharge relationships such as (1.3). We showed in [22] in particular that the results of our model successfully reproduced experimental results concerning gate behavior in a variety of situations, including situations where predictions based on the classical discharge relationship (1.3) were incorrect.

One of the further potentialities of our model was the possibility to take into account various types of flow perturbations, such as sediment transport and deposition along the canal. In the present paper, we couple various sedimentation processes to our LB model. These processes are mostly described by B. Chopard and his collaborators in previous works (see for instance [9, 11, 12, 27]). Our aim in this paper is to study how the form and structure of a sediment deposit evolves with time in the vicinity of an underflow gate, as well as how the flow around the gate is impacted by the presence of the deposit. Simulation results will be compared with data obtained from an experimental micro-canal, in order to validate the model. All this fits in the general context of studying how to adapt the LB method to irrigation canals modeling, in order to introduce its potential advantages in the field.

This paper is organized as follows. In Section 2, we will give a quick presentation of the canal model, the sedimentation algorithm, and how they were implemented and coupled. In Section 3, we propose a validation of the model, based on various experiments realized on the micro-canal of the ESISAR at Valence, France. Section 4 is dedicated to simulation results and Section 5 will provide some concluding remarks and present the potential perspectives of this work.

2 Model

The approach presented here is originally based on a bi-fluid Lattice Boltzmann model simulating an open irrigation canal which has been described in [22–26]. A sedimentation model was added to the original micro-canal model, which is based on the underlying physical processes described in [9, 11, 12, 27].

2.1 Lattice Boltzmann approach

The Lattice Boltzmann (LB) method is an alternative technique to standard methods based on partial differential equations for solving the Navier-Stokes equations. LB models are described in several textbooks or review papers. See for instance [1,3,6,7,30,31,35].

The Lattice Boltzmann method for hydrodynamics is a mesoscopic approach in which a fluid is described in terms of density distributions (also called distribution functions) usually noted $f_i(\mathbf{r},t)$ of idealized fluid particles moving and colliding on a regular lattice. Particles move on the lattice according to a set of possible velocities called $\mathbf{v}_i$, for $i=0,\cdots,z$, where z is called the lattice coordination number of the chosen lattice topology and $z+1$ is the number of discrete velocities. In one time step of the dynamics, particles move from one lattice site to another. A model topology is defined by its number of dimensions d and its number of velocities q and is noted DdQq. The quantities f_i's denote the density of particles entering a lattice site $\mathbf{r}$ at time t with velocity $\mathbf{v}_i$. In two-dimensional problems, the most used topology for Lattice Boltzmann models is the D2Q9, meaning there are nine elementary movement directions. The dynamic is composed of alternations of a propagation step during which a particle will move to the neighboring cell corresponding to its velocity, and a collision step during which the mass existing at a given site is redistributed between the density distributions accordingly to basic hydrodynamic principles.

Standard physical quantities such as particle density ρ, flow velocity $\rho\mathbf{u}$, and momentum tensor $\Pi_{\alpha\beta}$ can be defined by using the $f_i(\mathbf{r},t)$'s and $\mathbf{v}_i$'s to express momentums of various order of the distribution:

$$\rho(\mathbf{r},t)=\sum_i f_i(\mathbf{r},t),\quad \rho(\mathbf{r},t)\mathbf{u}(\mathbf{r},t)=\sum_i f_i(\mathbf{r},t)\mathbf{v}_i,\quad \Pi_{\alpha\beta}=\sum_i f_i(\mathbf{r},t)v_{i\alpha}v_{i\beta}. \tag{2.1}$$

The collision step of the Lattice Boltzmann dynamic consists in redistributing the mass on a lattice cell (i.e. changing the values of each density distribution $f_i(\mathbf{r},t)$) while respecting the adequate physical quantities (that is, most of the time, the particle density ρ and flow velocity $\rho\mathbf{u}$). Then, each density distribution of each cell is advected to the neighboring cell corresponding to its assigned elementary velocity. The collision operator (usually called Ω) may come in several forms. The most common one is the well-known single relaxation time model consisting in a relaxation equation in which one makes the density distributions $f_i(\mathbf{r},t)$ tend towards equilibrium density distributions. It is usually called Lattice BGK model because of its correspondence with the BGK form of the continuous

Boltzmann equation (see [4]). The relaxation equation reads:

$$f_i(\mathbf{r}+\Delta t\mathbf{v}_i,t+\Delta t)=f_i(\mathbf{r},t)+\frac{1}{\tau}\left(f_i^{eq}-f_i\right). \tag{2.2}$$

In this equation, τ is a relaxation time which is a free parameter of the model and is actually related to the viscosity of the fluid, and the f_i^{eq}'s are equilibrium density distributions that depend on the local density $\rho(\mathbf{r},t)$ and velocity $u(\mathbf{r},t)$, as well as on a number of model parameters. The main conditions that the f_i^{eq}'s must obey is that mass and momentum shall be conserved:

$$\sum_i f_i^{eq}=\sum_i f_i=\rho, \qquad \sum_i \mathbf{v}_i f_i^{eq}=\sum_i \mathbf{v}_i f_i=\rho\mathbf{u}. \tag{2.3}$$

These two conservation laws respectively correspond to the classical *continuity* and Navier-Stokes partial differential equations used in traditional fluid dynamics.

Using the properties of the velocity vectors $\mathbf{v}_i$, it can be shown (see [7,30,35]) that the following expression for f^{eq} satisfies the conservation laws (2.3):

$$f_i^{eq}=f_i^{eq}(\rho,\mathbf{u})=w_i\cdot\rho\cdot\left(1+\frac{v_{i\alpha}u_\alpha}{c_s^2}+\frac{1}{2c_s^4}\cdot(v_{i\alpha}v_{i\beta}-c_s^2\delta_{\alpha\beta})\cdot u_\alpha u_\beta\right), \tag{2.4}$$

where the w_i's are weights which depend on the lattice topology. For a D2Q9 model, $w_0=4/9$, $w_{1,3,5,7}=1/9$ and $w_{2,4,6,8}=1/36$. Note that in Eq. (2.4) as in what follows, we use Einstein summation convention over repeated Greek indices.

The behavior of the LB model (2.2) can be analyzed mathematically with, for instance a Chapman-Enskog method [7,8,21]. Several important results are obtained. It is found that, to order Δt^2 and Δx^2, and for small Mach number ($\mathbf{u}\ll c_s$), the LB dynamics implies that ρ and $\mathbf{u}$ obey the continuity and Navier-Stokes equation.

External forces $\mathbf{F}$ (usually called body forces) can also be added to a LB fluid. When $\mathbf{F}$ is constant is space and time, this can be done by adding a new term in Eq. (2.2). The new dynamics then reads:

$$f_i(\mathbf{r}+\Delta t\mathbf{v}_i,t+\Delta t)=f_i(\mathbf{r},t)+\frac{1}{\tau}\left(f_i^{eq}-f_i\right)+\frac{\Delta t}{v^2}\mathbf{v}_i\cdot\mathbf{F}. \tag{2.5}$$

Note that for non-constant body forces, several ways have been proposed in the literature to modify Eq. (2.2). A popular method is described in [18]. However, in the present work we shall still use (2.5), knowing that we may thus introduce slight deviation to the Navier-Stokes behavior when $\mathbf{F}=\mathbf{F}(\mathbf{r},t)$.

2.2 The canal model

We will use a Lattice Boltzmann model which allows us to describe a free-surface flow. The considered two-fluid LB model allows us to fully simulate a water-air system as it

has been shown in our previous works. This two-fluid model is based on the Shan-Chen model for immiscible fluids [28]. An interaction force is used to induce a separation between the two fluids, which leads to the creation of the free surface. A gravity force is also applied to the "water" fluid only (proportional to the local density of the fluid). Since we are using a Shan-Chen bi-fluid model, we name the two fluids "red fluid" and blue fluid" respectively with the red fluid will taking on the role of water and the blue fluid the role of air. Distribution functions of the water (red fluid) will therefore be addressed by $R_i(\mathbf{r},t)$, while distribution functions of the air (blue fluid) will be addressed by $B_i(\mathbf{r},t)$.

We use the well-known BGK equation for the collision operator (Bhatnager, Gross and Krook [4]). The relaxation equation reads, for instance for the water fluid:

$$R_i(\mathbf{r}+\Delta_r,t+\Delta_t)=R_i(\mathbf{r},t)-\frac{1}{\tau}(R_i(\mathbf{r},t)-R_i^{eq}(\mathbf{r},t))+\frac{m_i\Delta_t}{v^2C_2}v_i\cdot(F_R(\mathbf{r},t)+\vec{g_R}), \tag{2.6}$$

where the R_i are the density distributions of the fluid, τ is the relaxation time, F_R and $\vec{g_R}$ are resp. the air/water mutual interaction force and the gravity force (applied only on the water fluid).

When the two fluids are separated, the water fluid is mostly located at the bottom of the lattice, and the air fluid is mostly located at the top of the lattice. If we consider a column of cells of the lattice, it can roughly be divided in three parts: a part at the bottom where there is only water, a part at the top where there is only air and a transition part in between where both fluids are present. We call "water level" of the column the height for which the two fluids densities are equal (see the right-hand part of Fig. 1).

This model has some drawbacks. For instance, the full simulation of both fluids is costly and difference between the respective densities of both fluids cannot be too high. Free-surface LB models which do not require the explicit simulation of the gaz phase have been proposed [14–16, 19, 20]. We plan to consider these models in our future works.

The floor and walls of the system are modelled with bounce-back boundary conditions. Gates located at the boundaries of the system are modelled with modified pressure boundary conditions so that they recover the dynamics of the classical gate equation for an underflow submerged gate (a study of the modelling of gates in our model was realized in [22]). An "atmosphere" boundary condition is applied at the top boundary, which consists in setting a fixed pressure for the air fluid, and keeping the incoming almost-zero pressure of the air fluid (see the left-hand part of Fig. 1).

2.3 Sedimentation algorithm

In this model, the amount of granular particles on each lattice site is represented by an integer $n(r,t)$. These particles move on the same lattice as the LB fluid, and interact with it. They can exist in two states: free particles, and deposited (or frozen) particles.

The algorithm is made of several processes, which will manage the transport, deposition, erosion, and toppling of the particles.

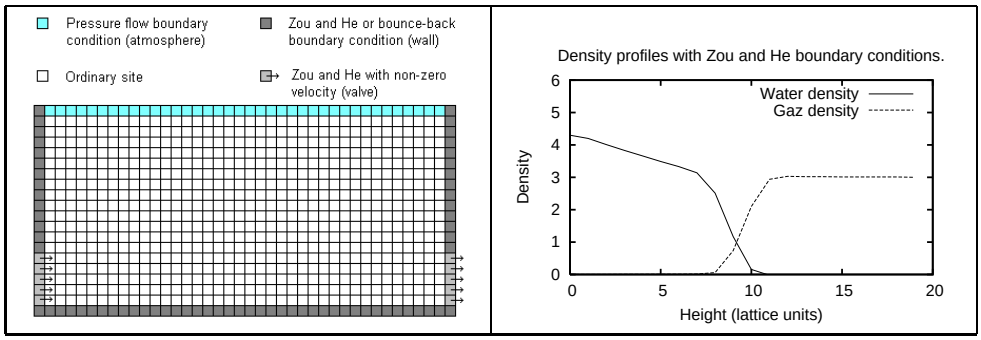

Figure 1: At left, the LB lattice for a one-reach system. At right, an example of a vertical density profile in the middle of a reach.

Transport algorithm: it defines the rules governing the motion of the free particles. The free particles move according to the direction of the fluid flow, but they are also subjected to the gravity force. Therefore, a free particle will be randomly moved to any neighboring site with a preferred direction determined by the vector $u+u_{fall}$, where u is the velocity of the fluid and u_{fall} is a "falling speed" directed toward the bottom of the lattice. The particle falling speed u_{fall} is used to determine whether particles will tend to crawl on the ground (strong u_{fall}) or be transported in suspension by the flow (low u_{fall}). For each direction i of the lattice, there is a probability of moving towards that direction which is proportional to the projection of the $u+u_{fall}$ vector on the v_i elementary movement vector. The transport process is also affected by a parameter τ_s which modify the probability of a particle to actually be moved to a neighboring site at each time step.

Deposition algorithm: when free particles in movement hit a solid boundary, they may become *frozen* (deposited) particles, which are no more subject to the transport process. Instead, they pile up until a certain threshold N_s is reached, or they can become again free particles if eroded. When the threshold value N_s is reached, the site becomes solid, creating a new boundary condition for the fluid around it. The deposition process is also parameterized by P_{sol}, which determines the probability of a moving particle to become a "frozen" particle when it is headed toward a solid site.

Erosion algorithm: it determines how frozen particles can change their state to become free particles. At each time step, each frozen particle on any given site has a probability of becoming a free particle which is proportional to the cumulated fluid velocities of the neighboring sites. The erosion process is parameterized by two quantities U_e (minimum flow speed for erosion to take place) and P_e (which affects the probability of erosion of particles).

Toppling algorithms: it describes mechanisms which have to be added since sediments usually do not have perfect cohesion. When a given site contains more frozen particles than one of its neighbors, it will give to this neighbors one of its own frozen particles only if the difference is at least equal to a given number δN, which actually determines

the slope of sediment deposits. This particle transfer only happens with a given probability, which sets the speed at which the toppling mechanism occurs. A second toppling mechanism ensures that a given site never has more frozen particles than the one located immediately below it, by transferring systematically all of the excess frozen particles.

Tuning and influence of sedimentation parameters: The most convenient way to control the time scale of sedimentation processes is to adjust the values of parameters P_{sol} and P_e while keeping constant the P_{sol}/P_e ratio. When these parameters are both high, the speed of both deposition and erosion processes will be high. On the other hand, if P_{sol} and P_e are low, the deposition and erosion processes will be slower. Changing the P_{sol}/P_e ratio will change respective importance of deposition and erosion, and will thus determine the overall importance of sedimentation in the system and the potential size of any deposit which might be formed (thus allowing to control the space scale of the sedimentation phenomena). Currently, we have not attempted to deduce from our sedimentation parameters a value for usual dimensionless numbers in the field (like, for example, the number of Shields [5, 29]). In many sedimentation models that are used classically in irrigation canals, two different transport modes for sediment particles [32] are considered: the bed load (particles rolling over the ground) and the suspended load (particles that are transported by the flow). In our model, we do not explicitly separate these two different transport modes as they naturally emerge from the mesoscopic description of our approach [9,11,12,27]: depending on the local flow condition and the sedimentation speed u_{fall}, particles will either crawl on the ground or move as suspension.

2.4 Implementation

The simulations were performed with a self-developed Lattice Boltzmann code written in C++. For each site, the following information must be known:

- Usual LB quantities: distributions functions, density and velocity of the fluid;
- Number of free particles (sedimentation);
- Number of frozen particles (sedimentation);
- Status - free or solid - of the cell (sedimentation).

At each time step, the global algorithm consists in applying first the usual LB processes (streaming and collision). Then, the densities and velocities for each cell are updated. The sedimentation processes are then applied. After sedimentation, the status of cells are updated: we have to keep track of cells which have changed their status (free or solid) because of sedimentation processes. At the next time step, LB processes will take into account these changes.

Compared to a simple LB simulation, a simulation with sedimentation processes will obviously take a longer time. This increment is variable: indeed, sedimentation processes will only take place in a given site if at least one sediment particle is present. Therefore,

the execution will depends on how particles are spread in the lattice. In the simulations presented in this paper, the execution time increment is generally comprised between 15% and 20%.

Cells status: Various methods for taking into account the cells status in the LB dynamic can be imagined. The most straight-forward one consists in treating a "solid" cell as an ordinary solid boundary, and applying a bounce-back boundary condition for this cell. However, in our case, important changes in LB density may happen due to changes in water levels. Thus, if a cell acquires the "solid" status when a given water level exists and loses this status when a significantly different water level is present, it could lead to an unwanted discontinuity of the density. Therefore, the preferred solution for treating the sedimented cells was to simply nullify the fluid velocity for this cell during the LB processes.

Sediment particles creation: The first possible source of sediments is simply the presence of a pre-existent deposit at the beginning of a simulation. In this case, a given number of sites have an initial number of frozen particles greater than the solidity threshold. These sites are initially considered solid. The second one is the creation of free particles at the lattice cells belonging to the gate located at the upstream end of the lattice. In the present work, only simulations using the first method will be used, since it corresponds to the micro-canal experiments set-up.

Discharge calculation: In the following work, we will have to calculate the discharge at the central gate. This quantity is not known directly, but has to be calculated from the LB density distributions at the gate cells. The usual expression for expressing a discharge in hydraulics (in the case of a mono-dimensional flow) is $Q = \int_S u(z)dzdy$, where the discharge Q is the amount of fluid (expressed in terms of mass of volume) that crosses the section S of the canal at each time unit, and $u(z)$ is the speed of a fluid particle at a given point. The usual local velocity in LB $u = (1/\rho)\cdot\sum_{i=1}^{z} v_i f_i$ is the mean movement speed of a particle on a given cell. In our initial trials, we attempted to use the local quantity ρu to keep track of the mass exchanges between a gate and a reach, but we observed that it did not give a correct measurement of the quantity of fluid that crosses a cell.

We calculate the discharge at the gate according to a specific formula expressing the quantity of fluid that crossed a section during one time step. We wish to obtain a balance of the mass exchanged between the gate cells and the reach located just after. The quantity we are looking for is the difference between the sum of the density distributions f^{in} entering gate cells from cells of the considered reach before the collision step of the LB dynamic, and the density distributions f^{out} leaving gate cells for cells of the considered reach after the collision step of the LB dynamic. If one considers a flow streaming from

left to right, one has:

$$Q=\sum_{y^{gate}=y^{gate}_{min}}^{y^{gate}_{max}}\Big[\Big(f_1^{out}(x^{gate},y^{gate})+f_2^{out}(x^{gate},y^{gate})+f_8^{out}(x^{gate},y^{gate})\Big) - \Big(f_4^{in}(x^{gate},y^{gate})+f_5^{in}(x^{gate},y^{gate})+f_6^{in}(x^{gate},y^{gate})\Big)\Big]. \tag{2.7}$$

Fig. 2 shows which density distributions must be taken into account for this calculation.

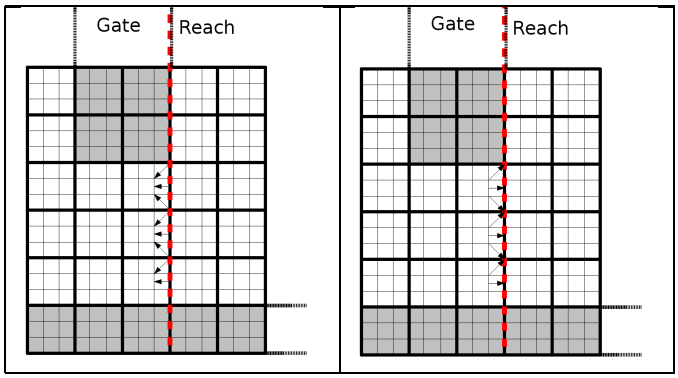

Figure 2: Directions associated with the density distributions taken into account for calculating the discharge at the gate (incoming populations before collision at left, outgoing populations after collision at right).

2.5 Model limitations, and experiment and simulation agreement

The bi-fluid LB model used in the present model has some important drawbacks that will justify its replacement with a more adapted LB model in the future. Notably, it requires that the two fluids have relatively similar densities, which is rather unadapted to our present case where we wish to simulate air and water. As a result, the obtained free surface dynamic is not expected to be realistic compared to real-life irrigation canals or even the micro-canal that was used for the experiment. In particular, the values of the dimensionless numbers traditionally used in hydraulics are much lower in our simulations than they were in experiments. Reynolds number were roughly comprised between 3000 and 14000 and Froude number between 0.25 and 3 for experiments, depending mostly on the gate opening; the values of these numbers in simulations were significantly lower (around or lower than unity for the Reynolds number, lower than 10^{-2} for the Froude number. For these reasons, the results we will present in this paper are qualitative since the model does not try to simulate a real-life, physical system. However, these early results obtained with our model when adding the sedimentation processes still show that it can capture some strong basic observable tendencies that were found in experiments realized on the micro-canal, despite the differences between the regimes and flow prop-

erties in simulation and experiments. Another drawback of the current bi-fluid model is the fact that fully simulating the two fluids obviously increases simulation times.

3 Model validation: behavior of a sediment deposit

The validation of the sedimentation model presented here relies on comparisons between simulation results and experiments on the micro-canal in Valence.

The micro-canal experiments were performed with a granular gravel-like material. This material density is quite high: when exposed to great variations of the local velocity of the fluid, the deposit will change shape or move along the floor of the canal and only a few particles will actually be eroded and swept away.

The experimentation protocol was set up according to these properties of the sediment. The simulation parameters were also chosen so that they reproduce the behavior that was observed during the experiments. An experiment essentially consists in placing a deposit of sediments around an underflow submerged gate, and then observe the influence of the deposit presence on the flow (such as perturbations of the discharge at the gate) and/or the behavior of this deposit (movement, deformations).

The experimental setup consists of an upstream pool whose water level is regulated, a downstream pool for water evacuation and the micro-canal divided by four gates (see Fig. 3). More precisely,

An outfall is located at the downstream end of the canal. It allows communication between the canal and the downstream pool.

The upstream and downstream gates (resp. gate 1 and gate 4) keep a constant opening during the experiment.

Upstream of the first gate, the water level is kept constant by an automatic regulation device maintaining a given water level in the upstream pool.

Gate 2 is manipulated during the experiments, and the sediment deposit is placed in its vicinity.

An additional gate (gate 3) is located between the downstream gate and the outfall in order to place a filter which prevents sediments from escaping the canal. The gate itself is kept wide opened during the experiments.

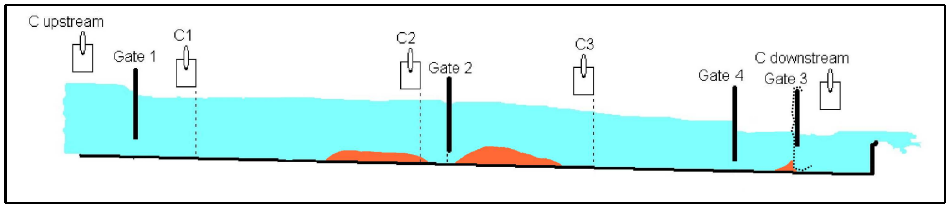

Figure 3: Micro-canal experiments: diagram of the experimental setup used for the sedimentation experiments. The sediment deposits are located around the studied gate (gate 2).

During micro-canal experiments, the initial sediment deposit was placed either on both sides of the gate (protocol 1), or on the downstream side only (protocol 2).

In protocol 1, Gate 2 is initially wide open. The deposit is manually placed for each new experiment, in presence of a water flow (which may be a difficult operation), so that its center corresponds to the location of Gate 2. The deposit is approximately 1 meter long and 3 centimeters high. In protocol 2, the deposit is only placed on the downstream side of the gate and is half the size it was in the first case. The gate is initially closed. This make the sediment deposit easier to set up in this case. In both cases, an experiment consists in adjusting the gate opening to a chosen value, and observe the response of the system (discharge, gate coefficient, movement and deformation of the deposit).

In LB simulations, the system is composed of three gates and two reaches (see Fig. 4). Two of the gates are located at the ends of the system and are modeled as boundary conditions reproducing the standard gate equation (1.3) for underflow immersed gates. The solid particles contained in the system are frozen particles forming the initial sediment deposit. There is not any arrival of solid particles through the upstream gate. The number of particles evacuated through the downstream gate will also remain negligible during the experiment.

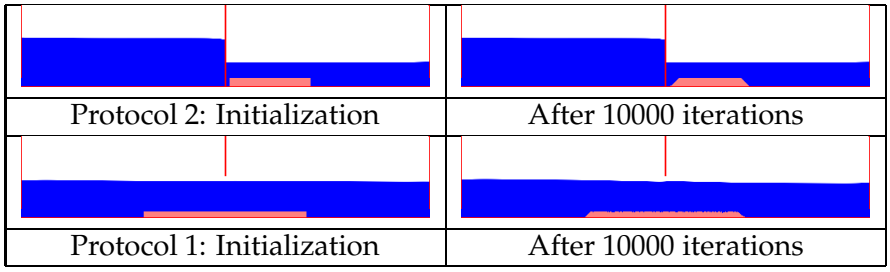

Figure 4: Initialization of the sediment deposit in simulations with both methods. Blue sites are sites where the fluid is present. Light red sites are sites where the number of frozen particles is high enough to consider this site as solid.

These constraints allow us to set the value of some model parameters:

u_{fall}: the falling speed of particles has to be strong enough to ensure that eroded particles fall back quickly to the sediment deposit instead of being evacuated downstream.

δN: this is the maximum difference between the number of frozen particles at two adjacent sites. This parameter determines the angle of repose of the deposit. In simulations, this angle has to fit approximately the angle observed in experiments.

Both initialization protocols were reproduced during LB simulations as illustrated in Fig. 4. The lattice sites containing solid sediment particles are represented in light red, while walls and canal floor are in red.

In this section, we consider the dynamic of the deposit. In particular, we will measure the evolution of the shape of the deposit and its distance to the gate as time goes on. The agreement between experiments and simulation will be interpreted as a qualitative

validation of the numerical model and its parameters. In the next section, we will study the influence of the a deposit on the gate dynamics.

3.1 Shape of the Deposit

We will first consider the micro-canal and observe sedimentation profiles obtained for several experiments. During each of them, the sediment deposit is placed according to protocol 1 (stationary flow, gate wide opened, deposit located both upstream and downstream of the gate). At the start of the experiment, the gate opening is reduced to a given value, and we wait for the deposit to stabilize before measuring its profile.

This experiment was repeated for three different openings of the gate, namely 6.2 cm, 5.3 cm and 3.6 cm. The profiles we observed are shown in Fig. 5 (profile *A* for a 6.2 cm opening, profile *B* for a 5.3 cm and profile *C* for 3.6 cm).

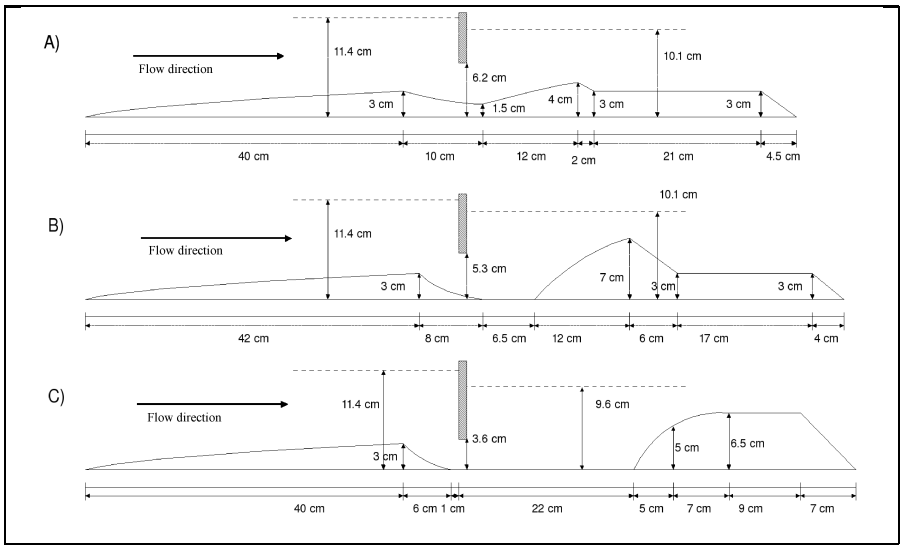

Figure 5: Micro-canal experiments: typical forms obtained for the sediment deposit for different gate openings.

The most interesting part of the deposit is observed in the downstream region, with respect to the gate. Three different classes of sedimentation profiles were observed:

A profile associated with high values of the gate openings (and therefore a low value for the local fluid velocity), characterized by the presence of a depression in the sediments under the gate (profile *A* in Fig. 5).

A profile corresponding to intermediate gate openings, characterized by the absence of sediments just under the gate, and a triangular shape downstream the gate (profile *B* in Fig. 5).

A profile associated with small values of the gate openings, where the triangular shape has spread to the entire deposit, forming a trapezoidal mass (profile *C* in Fig. 5).

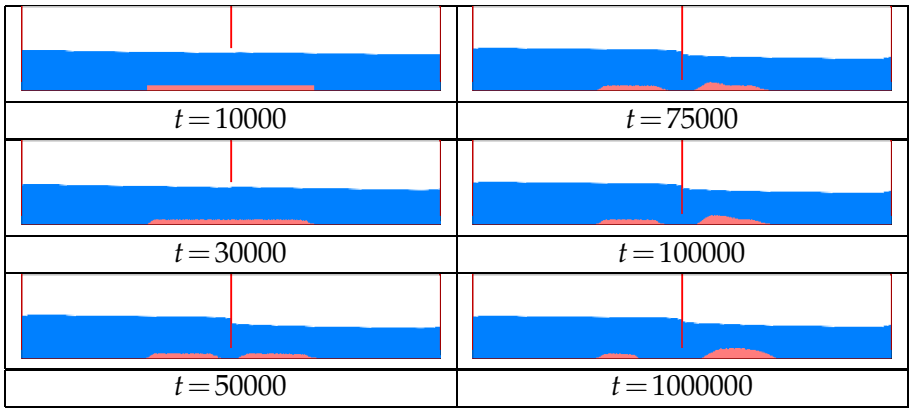

Figure 6: LB simulations: reproduction of the micro-canal experiments shown in Fig. 5. The sedimentation processes are launched at $t=10000$ iterations. At $t=50000$, the gate is partially closed. We show the system state at times 10000, 30000, 50000, 75000, 100000 and 1000000.

When the gate opening is small enough, the final state of the deposit is profile *C*, after transiting by the intermediate stage *B*. We also observe a progressive movement of the whole deposit in the downstream direction, at a lower time scale.

All these types of profiles have also been observed in LB simulations.

We show in Fig. 6 the system evolution during a LB simulation with sedimentation: initially, the gate is open so that it does not interfere with the flow, as in the case with the micro-canal experiments. At the beginning of the test, the gate is partially closed, and we observe the consequences on the sediment deposit.

We note a similarity between experiments and simulations concerning the evolution of the deposit over time: a hole is formed under the gate, a triangular shape appears downstream the gate, which progressively spreads to the rest of the deposit until an homogeneous trapezoidal form is reached.

We also remark in Fig. 6 that the movement of the deposit over time is much more limited in simulations than it was in the micro-canal experiments. This is explainable since in experiments the material used for the micro-canal has a low rugosity, while in simulations a no-slip boundary condition is imposed to the floor sites, hence producing a more rugose floor.

3.2 Movement of the deposit over time

A series of experiments was performed to study the evolution of the deposit over time, during which the distance between the gate and the sediments was periodically measured. The distance from gate to sediments was measured in *cm* in the experimental case, and in lattice sites number in the simulation case. In both cases, it is considered to be the distance between the gate and the nearest end of the deposit.

At the beginning of each experiment, the sediment deposit was placed again according to protocol 1. The left part of Fig. 7 shows the evolution of the distance between the

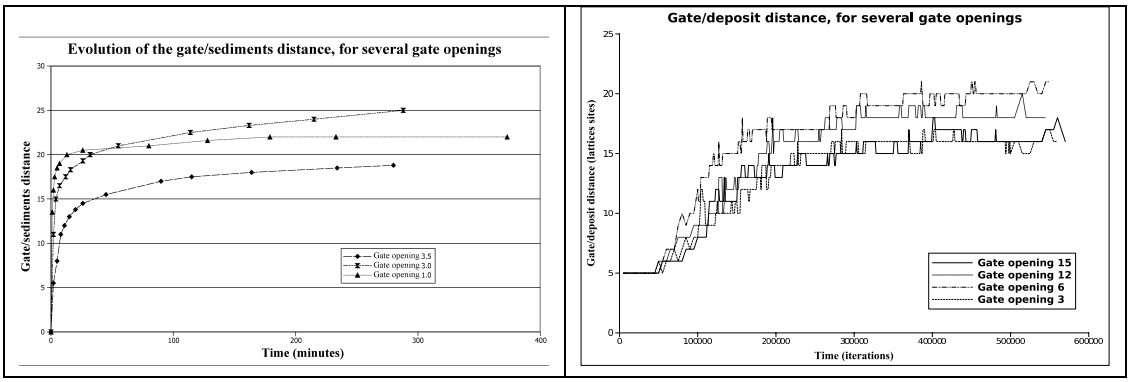

Figure 7: At left: micro-canal experiments – evolution of the distance between the sediment deposit and the gate over time, for several values of the gate opening. At right: LB Simulation – evolution of the gate/deposit distance.

sediment deposit and the gate, for several values of the gate opening (each distinct value means a different experiment).

Several observations can be made from these figures. When the gate opening is small, the initial speed of the deposit is high (see the 1.0 cm gate opening curve in Fig 7) but the gate/deposit distance quickly reaches a maximum. For higher gate openings, the speed is smaller and the final value of the gate/deposit distance could not be observed within the duration of the experiment.

We observed that the 3.5 cm gate opening curve is lower than the curve corresponding to a 3.0 cm opening, but that the 1 cm curve is roughly located between them. Therefore, we can make the assumption that the final gate/deposit distance is low for very small gate openings, increases when the gate opening increases, reaches a maximum value for a certain gate opening, and then decreases again.

We also measured the time evolution of the gate/sediments distance with the LB simulations. The gate opening (in lattice units) was changed at each simulation. The boundary condition used here for the floor was a bounce-forward one, ensuring a low friction force on the floor in order to be closer to the conditions of the micro-canal.

For the simulation we will show here, we chose a stationary initial state (the studied gate is initially wide opened and a stationary flow is present). The initial deposit is located only on the downstream side of the gate. When the experiment start, the gate is partially closed. Therefore, this protocol takes elements from both methods used in micro-canal experiments for establishing the deposit: the simulation starts while a steady flow exists in the canal like in protocol 1, but with sediments only on the downstream side like in protocol 2. This to prevent the gate from being blocked by sediments for small gate openings.

Results are shown in part right of Fig. 7, for gate openings of 3, 6, 12 and 15 lattice sites. There are minor differences between simulations and experiments: during micro-canal experiments, a test realized with a very small gate opening is characterized by an

important movement speed for the sediment deposit at the beginning of the experiment. This is not observed in simulations.

On the other hand, the observation we made on the micro-canal concerning the non-monotonic increase of the displacement of the deposit with the gate opening is well reproduced in the LB simulations. Fig. 7 (right-hand graphic) also shows that a gate opening of 12 or 15 exhibit a final gate/deposit distance which is smaller than that obtained with an opening of 6 lattice sites, which is itself larger than the distance observed with a 3 lattice sites opening.

4 Study of the sediment deposit influence on the dynamics of an underflow gate

The aim of this section is to study the influence of sediment on the amount of water that can flow through a gate. Two quantities were measured or computed during this study:

Discharge: during micro-canal experimentations, the discharge is measured at the outfall and recorded through the control software. When in steady flow, the discharge is supposed to be uniform over all the canal length (thus, the discharge at the gate can be assumed to be identical to the discharge at the outfall). During simulations, it is calculated directly from the distribution functions at gate sites.

Gate coefficient θ: it is calculated according to Eq. (1.3) from the measurement of the discharge Q, the gate opening O and water levels h_{up} and h_{down} before and after the gate.

4.1 Experiments on the micro-canal

We compare two sets of experiments: one without sediments, and the other one with sediments.

During a given set of micro-canal experiments, values for the discharge are measured at steady state for several values of the gate openings. In the case without sedimentation, the initial condition is a situation where the studied gate is wide opened. The gate opening is then reduced by stages, each time waiting for the stationary regime to measure the discharge.

During the tests with sedimentation, we used protocol 2 for placing the initial deposit, thus starting with a closed gate, and a deposit placed only on the downstream side.

Results are shown in Figs. 8 and 9 which show respectively the discharge and the gate coefficient θ, with and without sedimentation; experimentation results are shown on the left parts of these figures, while simulation results, which will be discussed later, are represented on the right parts. These results allow us to observe that both discharge and gate coefficients are reduced in presence of sediments, with the difference being less important for low gate openings (for large gate openings as well for the gate coefficient).

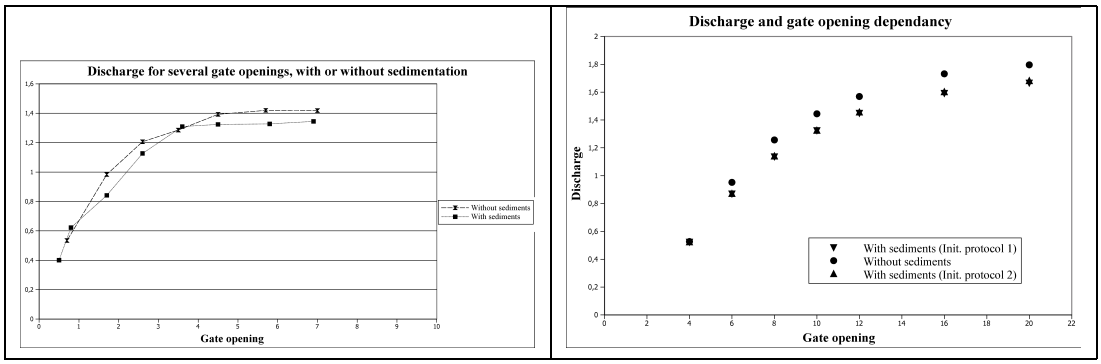

Figure 8: At left: Experiments on the micro-canal – discharge at equilibrium for several gate openings, with and without sedimentation. At right: LB simulation – discharge as a function of the gate opening for several tests realized with and without sedimentation.

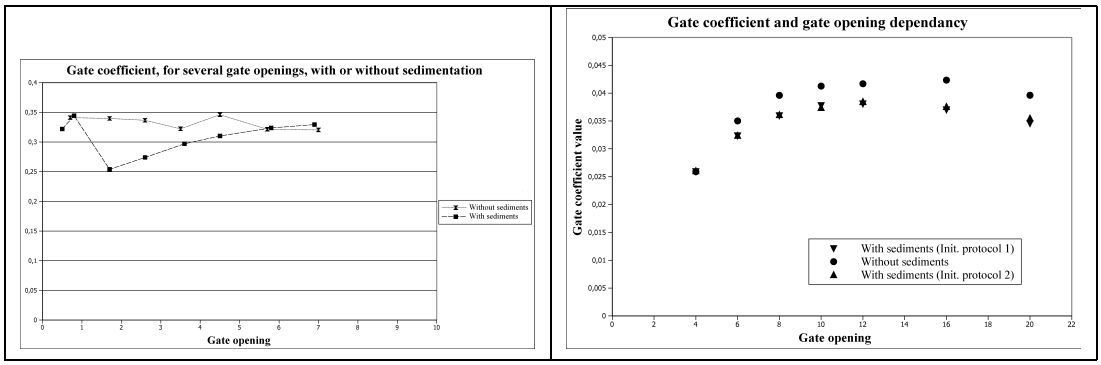

Figure 9: At left: Experiments on the micro-canal – gate coefficient at equilibrium for several gate openings, with and without sedimentation. At right: LB simulation – gate coefficient as a function of the gate opening for several tests realized with and without sedimentation.

4.2 Simulation results

The simulation system is made of two reaches separated by an internal gate which is the studied gate (see Fig. 6). At the upstream and downstream ends are two external gates which are given a constant opening during all simulations. Each test consists in starting from an initial situation with or without sediments (in cases with sediments, initialization protocols 1 or 2 may be used), set the gate opening to a given value, and then wait for the steady state.

The results of these simulations are given in the right-hand parts of Figs. 8 (for discharge) and 9 (for the gate coefficient). We can make several observations.

First, the existence of a sediment deposit clearly affects the discharge near the gate, as well as the gate coefficient.

Then, there is an almost perfect agreement between the results of the two initialization protocols. This is surprising, since there are a number of significant differences: the existence of an upstream deposit in the case of the protocol 1, and the fact that the total

quantity of sediments is more important in protocol 1 leading to a bigger deposit.

Finally, for small gate openings, there is little difference between the cases with and without sediments, as also observed in the micro-canal experiments.

5 Conclusion

In previous works [22–26], we designed a two-fluid water-air Lattice Boltzmann model with gravity forces modeling a free-surface irrigation canal. This model was shown to reproduce expected behaviors concerning shallow-water equations and gate dynamics. In the present paper, we have added the transport, erosion and deposition of sediments to our model.

The validation of this extended model through comparison between simulations and experiments realized on a micro-canal constitutes a significant part of the present work.

A good agreement between simulations and experiments was found. In both simulations and experiments, we studied the case of a sediment deposit placed on one or two sides of a given underwater gate. First, it was found that the evolution of the deposit profile during a simulation and the corresponding experiment was consistent. Strong similarities between experiments and simulations were also found when examining the evolution of the gate/deposit distance. Moreover, the influence of the presence of a deposit on the gate dynamics was also extremely similar between experiments and simulations: in both cases, the discharge at the gate was clearly affected by the presence of sediments.

The simulations presented in this paper focused on reproducing experiments on the micro-canal. However, it is possible to tune the parameters of the sedimentation algorithm in order to simulate other situations. For instance, other simulations have been run assuming a greater mobility for particles, and particle creation at the upstream gate. In this situation, particles can ”enter” the system via the upstream gate and leave it via the downstream one. A basic experiment in this situation consists in testing how much sedimentation is found in the central reach of a three-reach system depending on the opening of the two central gates. Results have been obtained which correspond to what is intuitively expected: there is more sedimentation in the system when the gate openings are small, and the dependency is more visible for the downstream gate.

Note that our model could also be extended to introduce the growth of algae and in canal bed.

The perspectives of this work are to apply the knowledge acquired concerning the sedimentation processes to the prediction of its possible consequences on the control systems operating the gates of an irrigation system.

References

[1] C. K. Aidun and J. R. Clausen. Lattice-boltzmann method for complex flows. Annu. Rev. Fluid Mech., 42:439–472, 2010.

[2] Bedrich Benes. Real-time erosion using shallow water simulation. In 4th Workshop in Virtual Reality Interactions and Physical Simulation, 2007.
[3] R. Benzi, S. Succi, and M. Vergassola. The lattice boltzmann equation: theory and applications. Physics Reports, 222:145–197, 1992.
[4] P. Bhatnager, E. Gross, and M. Krook. A model for collision process in gases. Phys. Rev., 94, 511, 1954.
[5] J.M. Buffington. The legend of a.f. shields. Journal of Hydraulic Engineering, April:376–387, 1999.
[6] S. Chen and G.D. Doolen. Lattice boltzmann method for fluid flows. Ann. Rev. Fluid Mech., 30:329–364, 1998.
[7] B. Chopard and M. Droz. Lattice-Gas Cellular Automata and Lattice Boltzmann Models: an Introduction. Cambridge University Press, 1998.
[8] B. Chopard, P. Luthi, A. Masselot, and A. Dupuis. Cellular automata and lattice boltzmann techniques: An approach to model and simulate complex systems. Advances in Complex Systems, 5-2:103–242, 2002.
[9] B. Chopard, A. Masselot, and A. Dupuis. A lattice gas model for erosion and particle transport in a fluid. In LGA'99 conference, Tokyo, volume 129, pages 167 – 176, 2000.
[10] Julie Dréano. Morphodynamique des rivières. PhD thesis, Université Rennes 1, 2009.
[11] A. Dupuis and B. Chopard. Lattice gas modeling of scour formation under submarine pipelines. Journal of Mathematical Physics, 178(1):161 – 174, 2002.
[12] A. Dupuis and B. Chopard. Lattice gas simulation of sediments flow under submarine pipeline with spoilers. In The 4th international conference on HydroInformatics, Cedar Rapids, USA, 2002.
[13] L. Fraccarollo1, H. Capart, and Y. Zech. A godunov method for the computation of erosional shallow water transients. Int. J. Numer. Meth. Fluids, 41:951–976, 2003.
[14] Irina Ginzburg. Equilibrium-type and link-type lattice boltzmann models for generic advection and anisotropic-dispersion equation. Advances in Water Resources Pages, 28-11:1171–1195, 2005.
[15] Irina Ginzburg. Lattice boltzmann modeling with discontinuous collision components: Hydrodynamic and advection-diffusion equations. J. Stat. Phys., 126-1:157–206, 2007.
[16] Irina Ginzburg and Konrad Steiner. Lattice boltzmann model for free-surface flow and its application to filling process in casting. Journal of Comp. Physics, 185:61–99, 2003.
[17] Christopher Groh, Ingo Rehberg, and Christof A. Kruelle. Particle dynamics of a cartoon dune, 2009.
[18] Z. Guo, C. Zheng, and B. Shi. Discrete lattice effects on forcing terms in the lattice boltzmann method. Phys. Review E, 65:046308–046313, 2002.
[19] C. Körner, T. Pohl, U. Rüde, N. Thürey, and T. Hofmann. Lattice boltzmann methods with free surfaces and their application in material technology. Technical report, Friedrich-Alexander-Universitaä Erlangen-Nürnberg - Institü Fur Informatik (Mathematische Maschinen und Datenverarbeitung), 2004.
[20] C. Körner, M. Thies, T. Hofmann, N. Thürey, and U. Rüde. Lattice boltzmann model for free surface flow for modeling foaming. Journal of Statistical Physics, Nos. 1/2, 121, no 1/2, 2005.
[21] Jonas Lätt. Hydrodynamic Limit of Lattice Boltzmann equations. PhD thesis, University of Geneva, Switzerland, 2007.
[22] O. Marcou, B. Chopard, S. El Yacoubi, B. Hamroun, L. Lefèvre, and E. Mendes. Lattice boltzmann models for simulation and control of unsteady flows in open channels. Journal

of Irrigation and Drainage Engineering, 2009.
[23] O. Marcou, S. El Yacoubi, and B. Chopard. A bi-fluid lattice boltzmann model for water flow in an irrigation channel. In ACRI 2006 Proceedings., pages 373–382. Springer, 2006.
[24] O. Marcou, S. El Yacoubi, and B. Chopard. Modélisation d'un canal d'irrigation par la méthode de boltzmann sur réseaux. In Conférence Internationale Francophone d'Automatique 2008, 3-5 Septembre, Bucarest, Roumanie, 2008.
[25] O. Marcou, S. El Yacoubi, B. Chopard, and L. Lefèvre. Validation of a lattice boltzmann model for irrigation canals. In The Fifth International Conference on Mesoscopic Methods in Engineering and Science, ICMMES, 16-20 Juin, Amsterdam, Pays-bas, 2008.
[26] Olivier Marcou, B. Chopard, and S. El Yacoubi. Modeling of irrigation canals: a comparative study. Int. J. Mod. Phys. C, 18 (4):739–748, 2007.
[27] A. Masselot and B. Chopard. A lattice boltzmann model for transport and deposition. Europhysics letters, 100(6), 1998.
[28] X. Shan and H. Chen. Lattice boltzmann model for simulating flows with multiple phases and components. Phys. Review E, 47, no 3, 1993.
[29] A. Shields. Anwendung der aehnlichkeitsmechanik und der turbulenzforschung auf die geschiebebewegung. Mitteilungen der Preuischen Versuchsanstalt für Wasserbau, 26, 1936.
[30] Sauro Succi. The Lattice Boltzmann Equation, For Fluid Dynamics and Beyond. Oxford University Press, 2001.
[31] M.C. Sukop and D.T. Thorne. Lattice Boltzmann Modeling: an Introduction for Geoscientists and Engineers. Springer, 2005.
[32] Nestor J. Mendez V. Sediment transport in irrigation canals. A. A. Balkema publishers, 1998.
[33] A. Valance and V. Langlois. Ripple formation in weakly turbulent flow. Eur. Phys. Journ. B, 43:283–294, 2002.
[34] A. Wierschem, C. Groh, I. Rehberg, N. Aksel, and C.A. Kruelle. Ripple formation over a sand bed submitted to a laminar shear flow. Eur. Phys. Journ. E, 25:213–221, 2005.
[35] Dieter A. Wolf-Gladrow. Lattice-Gas Cellular Automata and Lattice Boltzmann Models: An Introduction. Lecture Notes in Mathematics. Springer, 2000.